NATIONAL ADVISORY COMMITTEE FOR AERONAUTICS

TECHNICAL NOTE

No. 1316

THEORETICAL AERODYNAMIC COEFFICIENTS OF

TWO-DIMENSIONAL SUPERSONIC BIPLANES

By W. E. Moeckel

Flight Propulsion Research Laboratory
Cleveland, Ohio

Washington
June 1947

NATIONAL ADVISORY COMMITTEE FOR AERONAUTICS

TECHNICAL NOTE NO. 1316

THEORETICAL AERODYNAMIC COEFFICIENTS OF

TWO-DIMENSIONAL SUPERSONIC BIPLANES

By W. E. Moeckel

SUMMARY

The effect of varying the design of supersonic biplanes has been
theoretically investigated to determine the configuration required
for optimum aerodynamic performance. The investigation was chiefly
concerned with biplanes having lower and upper airfoils of equal chord
length and of triangular cross section. For such biplanes the changes
in aerodynamic performance resulting from varying the edge angles
simultaneously and in pairs were calculated. Lift and drag coeff-
cients were also calculated for a biplane having convex sections and
for a configuration employing a small shock-reflecting surface in
place of the lower airfoil.

The theoretical aerodynamic coefficients of the biplanes inves-
tigated are compared with those of an airfoil with diamond profile
and with those of a thin flat plate. The variation of the center of
pressure with angle of attack and the relative loading of the airfoils
was also investigated for several biplanes. For one biplane of
triangular cross section, the variation of the aerodynamic coefficients
with flight Mach number was calculated. A discussion of the effects
of friction drag on the relative performance of biplanes and single
airfoils is included.

The calculations show that, in a frictionless supersonic air
stream, biplanes of triangular cross section yield higher lift-drag
ratios than diamond airfoils of the same thickness ratio and that,
for high lift coefficients, unsymmetrical biplanes yield higher lift-
drag ratios than symmetrical biplanes. When friction drag is con-
sidered, the calculations show that biplanes with the lower airfoils
thicker than the upper airfoils should have higher lift-drag ratios
than symmetrical biplanes.

For each of the biplanes an optimum spacing was found at each
Mach number. Although the performance of the biplanes for this optimum
spacing was found to be improved over that of a diamond airfoil, the
calculations showed that with a constant biplane spacing this improve-
ment was maintained over only a limited range of Mach numbers near the
optimum.

INTRODUCTION

At supersonic speeds in a frictionless fluid the aerodynamic shape with the least drag and the greatest lift-drag ratio is the thin flat plate. Practical airfoils, however, must have finite thickness and consequently will have lower lift-drag ratios than the thin flat plate. For a given finite thickness ratio the lowest drag and the greatest lift-drag ratio are obtained with airfoil sections having a diamond profile (fig. 1(a)). The aerodynamic performance of a diamond airfoil, however, may theoretically be exceeded by means of a proper superposition of two airfoils of triangular cross section (fig. 1(b)). The possibility of using such arrangements to approximate the aerodynamic characteristics of a thin flat plate was suggested by Busemann in reference 1. An analysis of such biplanes was undertaken by Walchner in reference 2. As a first approximation, the pressures on the inner surfaces of certain properly shaped biplanes were shown to be mutually canceled and only the outer two surfaces were shown to contribute to the wave drag. These two surfaces are equivalent to those of a thin flat plate. Busemann's approximation, however, assumes that the expansion around the inner corners (fig. 1(b)) takes place across a single discontinuity plane; whereas the expansions actually occur through a wedge-shaped region. A part of the expansion wave from each of the inner corners is thus intercepted by the rear surface of the opposite airfoil and the rest passes outside the biplane. (See fig. 2.) The pressures are therefore not equalized internally and transition to free-stream conditions must take place externally by means of compression shocks. These transitions represent energy losses that appear as increases in the drag of the biplane arrangements.

Walchner (reference 2) showed that the expansion waves can be completely contained within a biplane if the trailing-edge contours are so curved that the rarefaction waves are not reflected from the surfaces. The required contour, which has zero trailing-edge angles, is incompatible with the strength requirement of practical wings. Walchner integrated the theoretical pressures over the surfaces of two possible biplane arrangements to determine the extent to which the drag and lift coefficients are altered when nonzero edge angles are maintained. He concluded that when friction drag was considered these biplanes were approximately equal in drag to a biconvex airfoil of the same thickness as one of the airfoils of the biplane.

An experimental investigation of a symmetrical supersonic biplane was reported by Ferri (reference 3). The optical observations reported indicate that the starting characteristics of supersonic biplanes are in many ways similar to those of a convergent supersonic diffuser. When the speed of the airstream past the biplane was increased from

subsonic to supersonic values, with the spacing between the two air-
foils set at the theoretical optimum value, the theoretical shock
configuration was not obtained. Instead, fluctuating shock configur-
ations were observed until the design velocity was reached; then a
shock wave curved inward from the leading edges was observed to span
the entrance between the two airfoils. When the spacing between the
airfoils was slightly increased the expected intersecting oblique
shock pattern appeared and remained when the spacing was again reduced
to optimum. Ferri found that when the curved-shock configuration was
present the drag of the biplane was about six times as great as when
the theoretically expected shock configuration was attained. A
probable solution to the problem of reaching optimum operating condi-
tions is a starting rocket to accelerate the aircraft to or beyond
its design Mach number. For wind-tunnel investigations, of course,
the spacing may be made variable and adjusted to its optimum value
only after the design Mach number is attained.

The present theoretical investigation was undertaken to deter-
mine the effect of design variations and operating variables on the
aerodynamic performance of biplanes. The design variations for
triangular-section biplanes included (1) variation of all edge angles
simultaneously, (2) variation of the edge angles of the lower and
upper airfoils separately, and (3) separate variation of the trailing-
edge angles. Lift and drag coefficients were also calculated for a
biplane having circular convex sections and for a configuration
having a small shock-reflecting surface in place of the lower airfoil.
The calculated aerodynamic coefficients are compared with those of a
diamond airfoil and with a thin flat plate. The variation of the
center of pressure with angle of attack was investigated for a
symmetrical and an unsymmetrical biplane, and the loading of these
biplanes was compared with that of a diamond airfoil. For one
biplane, the variation of aerodynamic coefficient with Mach number
was also determined. The effect of friction drag on the relative
performance of the biplanes and single airfoils is discussed.

DESCRIPTION OF BIPLANE ARRANGEMENTS

The biplanes investigated are chiefly of the type shown in fig-
ure 1(b), that is, biplanes consisting of two triangular-section
airfoils of equal chord length. The terms used in discussing such
biplanes are defined in the figure. The corresponding terms for
comparison with the diamond airfoil are defined in figure 1(a). From
the definition of thickness ratio, a diamond airfoil with the same
edge angle as the thinner of the airfoils of the biplane has the same
thickness ratio as that biplane.

For optimum performance, the spacing between the two airfoils of a triangular-section biplane $(d/c)_{opt}$ is determined by the requirement that the shocks from the leading edges shall intersect the surface of the opposite airfoil at the inner turning corner. This optimum spacing varies with free-stream Mach number M_0 and with leading-edge angle θ_1, as shown in figure 3. The variation of optimum spacing with angle of attack was found to be slight and is not indicated on this figure. Optimum spacing was assumed throughout the calculations with the exception of those reported in the discussion of the effect of varying the Mach number with constant spacing.

Whether the biplane was rotated as a whole about a fixed axis or each airfoil was separately rotated about its leading edge, as in figure 1(b), was found to be immaterial in determining the effect of angle of attack on biplane performance. The configuration with leading edges on a common vertical line was assumed in the calculations.

METHOD OF CALCULATION

The following symbols are used in the discussion and the figures:

c   chord

C_D drag coefficient for nonviscous flow

$C_{D,f}$ friction-drag coefficient

C_L lift coefficient

C_m pitching-moment coefficient around leading edge

C_p center-of-pressure coefficient, e/c

d   distance between airfoils of a biplane

d/c biplane spacing

e   distance from pitching-moment axis to center of pressure

$k = \left(\dfrac{\gamma-1}{\gamma+1}\right)^{\frac{1}{2}}$

M   Mach number

P   total pressure

p   static pressure

t   maximum thickness (of thinner airfoil for biplanes)

t/c thickness ratio

α angle of attack

β Mach angle

γ ratio of specific heats

θ edge angle

λ angle between local flow direction and free-stream flow
        direction

φ angle between shock and flow direction ahead of shock

Ψ angle through which flow is turned (Prandtl-Meyer theory)

Subscripts:

U   upper

L   lower

0   free-stream

1   leading

2   trailing

opt   optimum values

An analysis of the flow through triangular-section supersonic
biplanes is presented in the appendix. Such an analysis shows that
as the air passes between the airfoils it is first abruptly com-
pressed by the deflection due to the leading edges and then expanded
around the inner turning corners. The aerodynamic coefficients of
the biplane are obtained by determining the pressure distribution on
the surfaces resulting from compression and expansion. The expansion
process is readily followed with the help of the Prandtl-Meyer theory
of flow around corners (reference 4). This theory gives the ratio of
static to total pressure p/P, Mach number M, and Mach angle β
as functions of the angle through which the flow is turned Ψ. These
relations, where Ψ is taken equal to 0 for $M = 1.0$, are plotted
in figure 4.

The compressive turning at the leading edges takes place through oblique shocks; the direction of these shocks is determined by the Mach number of the free stream and by the angle of inclination of the biplane surfaces to the free-stream direction. The pressure resulting from such compressive turning may be determined from oblique-shock relations. The Prandtl-Meyer relations, however, give sufficiently good approximations to pressure resulting from compressive turning if the shocks are not too intense; that is, if the process is approximately isentropic. For the angles of inclination and the Mach numbers considered in the present investigation, errors resulting from the use of the Prandtl-Meyer theory in place of exact oblique-shock relations to determine pressures resulting from compressive turning were found to be insignificant. This theory was therefore utilized for convenience in calculation to determine all pressures as well as Mach lines. The angles between the shocks and the flow directions, which determine the optimum distance between the airfoils, differed considerably from the Mach angles assumed by the Prandtl-Meyer theory and were therefore obtained from exact oblique-shock relations.

The pressure distribution on the biplane surfaces may be obtained either by graphical or by analytical integration. Because the integration process is rather laborious, an analytical method suitable for solution with computing machines was developed. This method is described in the appendix.

An example of the graphical determination of pressure distributions is given in figure 2. The angle Ψ that determines the pressure ratio p/P, the Mach number M, and the Mach angle β is indicated in each region together with the angle between the local flow and the free-stream flow λ. The continuous-expansion regions have been replaced by successions of Mach lines, each of which turns the flow through an angle of 1^{O}. The expressions giving the intercepts of these Mach lines on the biplane surfaces in terms of local Mach angles are given in the appendix.

In the calculation of the aerodynamic coefficients, the following simplifying assumptions were made: (1) The continuous-expansion regions can be replaced by a succession of Mach waves, each of which expands the flow through an angle of 1^{O}; (2) these Mach waves are abruptly deflected at a definite point in the interaction region (see appendix); and (3) additional drags due to viscosity will be additive. With regard to the first two assumptions, it was felt that the small additional accuracy to be expected from assuming smaller expansion intervals or plotting the interaction region more carefully did not warrant the additional labor required. The third assumption implies that the calculated values of C_L are correct for viscous,

as well as nonviscous, air flow and that the friction-drag coefficient $C_{D,f}$ may be experimentally determined from the difference between the total drag coefficient and the drag coefficient calculated for non-viscous flow C_D.

At high Mach numbers the ratio of static to total pressure p/P becomes very small (fig. 4) and the differences between p/P on the front and rear or the top and bottom surfaces of an airfoil, which determine the aerodynamic coefficients, are of the order 10^{-3} for Mach numbers greater than about 3.5. For high Mach numbers, there-fore, the accuracy of calculated aerodynamic coefficients is chiefly limited by the low values of p/P. For this reason, few calculations were made for $M_0 > 3.0$.

If the thickness ratio of the airfoils is very small (values of $\theta < 4^\circ$), the variation of C_L and C_D of a supersonic biplane with Mach number and angle of attack may be determined approximately by means of simple equations given in reference 5. These equations were derived on the assumptions that the expansion around the inner corners takes place across a single discontinuity plane, that the variation of pressure with flow angle is linear, and that there is no deflection of the compression and expansion waves at their inter-section points. If the biplane spacing is optimum, the equations reduce to those obtained for a thin flat plate.

EFFECT OF VARYING EDGE ANGLES

The effect on drag and lift-drag ratio C_L/C_D of varying the edge angles θ of triangular-section biplanes is shown in figure 5. The values shown are for the optimum spacings $(d/c)_{opt}$ presented in figure 3. Figure 5(a) shows the effect of simultaneously varying all edge angles. Calculations were made for three free-stream Mach numbers M_0 and for angles of attack α of 0° and 3°. For $M_0 = 1.6$ the calculations were carried out only for $\theta < 7^\circ$ because the flow between the airfoils becomes subsonic when $\theta > 7.3^\circ$ and the supersonic-biplane theory no longer applies. The lift-drag ratio C_L/C_D is seen to be almost independent of Mach number for the optimum spacings assumed.

The effect of varying only θ_U while θ_L is held constant at 10° is shown in figure 5(b). Curves are shown for values of M_0 of 2.0 and 3.0 at an α of 0° and for an M_0 of 3.0 at an α of 3° For these conditions C_L/C_D reaches an optimum for a θ_U of about 5°. Lift is obtained at an α of 0° when θ_U is somewhat smaller

than θ_L because an unsymmetrical flow exists between the airfoils,
which results in a greater average pressure on the upper airfoil than
on the lower airfoil. As θ_U is reduced below the optimum, the drag
begins to increase more rapidly than the lift and C_L/C_D again drops.

The effect of increasing θ_L while holding θ_U constant is
shown in figure 5(c) for a θ_U of 7°. Curves are drawn for an M_O
of 3.0 and for an α of 0° and 3°. For $\alpha = 3^O$, C_L/C_D remains
almost constant for $\theta_L < 10^O$, and decreases for larger θ_L. For
$\alpha = 0^O$, C_L/C_D rapidly increases as the value of θ increases to
8.5^O and then drops slightly for larger angles.

The effect of varying the value of θ_2 while θ_1 is held con-
stant at 10° is shown in figure 5(d). The optimum value in this case
again is the result of opposing tendencies: As θ_2 decreases, the
expansion around the inner corners becomes less and the average pres-
sures on the rear inner surfaces tend to increase. The expansion
waves from the inner corners, however, are intercepted by increasingly
larger portions of the inner rear surfaces, and lower pressures toward
the trailing edges result. Because the first tendency lowers drag and
the second tendency increases drag, an optimum value of θ_2 results.

COMPARISON OF POLAR DIAGRAMS

For comparison with the diamond airfoil and with the thin flat
plate, two biplanes were chosen from figure 5 and their drag and lift
coefficients were calculated for several additional angles of attack.
The results are plotted in figure 6. Comparisons are made at free-
stream Mach numbers M_O of 2.0, 3.0, and 4.0 in figures 6(a), 6(b),
and 6(c), respectively. The biplanes selected were a symmetrical
biplane with all edge angles $\theta = 7^O$ and an unsymmetrical biplane
with $\theta_U = 7^O$ and $\theta_L = 10^O$. The curves show that both biplanes
give greater lift for a given drag than a diamond airfoil of the same
thickness ratio for all values of α and M_O considered. For the
biplanes, the symmetrical configuration gives greater lift for a given
drag over the lower range of C_L; whereas for high values of C_L the
unsymmetrical configuration has lower drag than all others including
the thin flat plate. (For an M_O of 4.0 it was considered unnecessary
to calculate the polar diagram for the symmetrical biplane, inasmuch as
the relative position of the four configurations considered seems to be
insensitive to Mach number.)

The comparisons presented in figure 6 indicate that the unsymmetrical biplane has lower drag than the symmetrical biplane for high values of C_L. The maximum value of C_L/C_D obtainable (slope of a straight line from the origin tangent to the polar curve), however, is somewhat less for the unsymmetrical biplane. A polar curve for a biplane with a θ_U of 7° and a θ_L of 13° was calculated to determine whether this maximum value of C_L/C_D is reduced or increased by further increases in the values of θ_L (fig. 7). The trend toward greater values of C_L/C_D at high values of C_L is continued but the maximum value of C_L/C_D is reduced as the value of θ_L is increased.

The same three biplanes are compared in figure 8 with diamond airfoils of three thickness ratios and with a thin flat plate. In this figure C_L/C_D (which is substantially independent of M_0) is plotted against α. The symmetrical biplane and the biplane with a θ_L of 10° have maximum values of C_L/C_D greater than the symmetrical-diamond airfoil with values of θ of 5°; that is, for a given value of t/c the biplanes in frictionless flow have considerably greater lift-drag ratios than the symmetrical-diamond airfoil.

VARIATION OF CENTER OF PRESSURE

In order to determine the center of pressure of the biplanes compared in figure 6, their pitching-moment coefficients about the midpoint between the two leading edges were calculated. The center-of-pressure coefficient was then obtained from the relation $C_p = e/c = C_m/C_L$, where c is the chord length and e is the distance from the pitching-moment axis X to the center of pressure. (See fig. 9.) This ratio is plotted against α for the two biplanes of figure 6 and for the diamond airfoil of the same thickness ratio. The values of C_p were found to be substantially independent of Mach number for the biplanes as well as for the diamond airfoil. The value of C_p varies widely with α for the unsymmetrical biplane but is almost constant for the symmetrical biplane and for the diamond airfoil.

EFFECT OF VARYING MACH NUMBER WITH CONSTANT BIPLANE SPACING

The results presented thus far have dealt with biplanes of optimum spacing, which varies only slightly with angle of attack but quite widely with free-stream Mach number. Ferri (reference 3) found that, when the biplane spacing was less than or greater than optimum, the observed flow patterns differed greatly from those theoretically predicted. The high pressure beyond the intersection of the oblique shocks (fig. 2) was apparently transmitted through the boundary layer and resulted in a flow separation either ahead of or after the inner

turning corners, depending on whether the spacing was less than or greater than optimum. The oblique shocks did not strike the wing surfaces but were reflected as expansion waves from the separated fluid layer near the surfaces. The experimentally determined lift and drag coefficients were nevertheless found to vary with biplane spacing much in the manner predicted by theory (see fig. 55, reference 3) although the experimental variations were less than the theoretical.

Calculations were made to determine, at least qualitatively, the effect of varying the value of M_0 while a constant value of d/c was maintained. The biplane selected was the unsymmetrical one with $\theta_U = 7^O$ and $\theta_L = 10^O$. (The analytical integration method described in the appendix applies only when the shocks intersect the biplane surfaces at the inner turning corners; consequently, the pressure distributions for nonoptimum spacings had to be determined graphically.) The variation of drag coefficient C_D, center-of-pressure coefficient C_p, and lift-drag ratio C_L/C_D with Mach number for this biplane is shown in figure 10. The biplane spacing d/c was held constant at a value of 0.15, which is optimum for this biplane at a value of M_0 of 3.0. (See fig. 3.) Calculations were made for values of α of 3° and 5°. The curves show that, for these values of α, C_L/C_D remains greater than that of the diamond airfoil of the same thickness ratio for a range of Mach numbers between 2.7 and 3.4. Inasmuch as experimental variations were less than theoretical (reference 3), the actual range of Mach numbers for which C_L/C_D remains greater for the biplane than for the diamond airfoil will probably be wider than that indicated in figure 10.

RELATIVE LOADING OF BIPLANES AND DIAMOND-PROFILE AIRFOILS

Because the internal pressure in a biplane is considerably greater than atmospheric, the upper airfoil of a biplane may be expected, for a given lift, to be more heavily loaded than a single airfoil. The relative loading is shown in figure 11. The loading factor $\Delta(p/P)$ plotted in this figure is the difference between the average ratio of static to total pressure on the upper and lower surfaces of the airfoils. This factor is plotted against lift coefficient C_L for a symmetrical biplane, an unsymmetrical biplane, and a diamond airfoil for free-stream Mach numbers M_0 of 2.0 and 3.0. At the lower value of M_0, the unsymmetrical biplane is more heavily loaded; whereas at an M_0 of 3.0 the two biplanes are about equally loaded. Both biplanes are more heavily loaded than the diamond airfoil of equal thickness ratio except at very high lift coefficients.

The heavier loading of the biplanes, however, is probably no serious disadvantage; it should be feasible in practice to strengthen the biplanes by fastening the two airfoils together in some manner.

EFFECT OF FRICTION

Inclusion of friction effects should somewhat reduce the relatively greater lift-drag ratio of biplanes as compared with single airfoils, inasmuch as the additional drag due to friction will be about twice as great for the biplanes. No adequate data on friction-drag coefficients $c_{D,f}$ at supersonic speeds are yet available. The magnitude of the $c_{D,f}$ that will reduce the lift-drag ratio of the biplane to that of the diamond-profile airfoil may be estimated. If $c_{D,f}$ is assumed to be twice as great for biplanes as for single airfoils, the diamond airfoil will have a lift-drag ratio equal to that of a biplane when

$$\frac{c_{L,b}}{c_{D,b} + 2c_{D,f}} = \frac{c_{L,d}}{c_{D,d} + c_{D,f}}$$

or when

$$c_{D,f} = \frac{c_{L,b} \, c_{D,d} - c_{L,d} \, c_{D,b}}{2c_{L,d} - c_{L,b}}$$

where subscripts b and d indicate the biplane and the diamond airfoil, respectively. A few limiting values of $c_{D,f}$ were calculated from the curves of figures 6 and 7. Lift coefficient c_L and drag coefficient for frictionless flow c_D were calculated for the points of maximum c_L/c_D for values of M_0 of 2.0 and 3.0. The results appear in the following table:

	θ_L (deg)	C_L/C_D	C_D	$C_{D,f}$
$M_0 = 2.0$				
Diamond airfoil, $\theta = 7^\circ$		8.15	0.0164	
Biplane, $\theta_U = 7^\circ$	7	14.7	.0061	0.0037
Biplane, $\theta_U = 7^\circ$	10	14.0	.0092	.0063
$M_0 = 3.0$				
Diamond airfoil, $\theta = 7^\circ$		8.15	0.0111	
Biplane, $\theta_U = 7^\circ$	7	14.2	.0034	0.0017
Biplane, $\theta_U = 7^\circ$	10	13.2	.0072	.0042
Biplane, $\theta_U = 7^\circ$	13	10.5	.0142	.0330

An examination of this table shows that a greater value of $C_{D,f}$ is allowable for low values of M_0 and for large values of θ_L. These results indicate that, for a given value of t/c, the unsymmetry of the biplane should be increased the higher the friction coefficient encountered.

Similar calculations may be made to determine the limiting values of $C_{D,f}$ above which the unsymmetrical biplane has a lift-drag ratio higher than that of the symmetrical biplane. Calculations using the same values of C_L and C_D as in the table show that for an M_0 of 2.0 the biplane with $\theta_L = 10^\circ$ will yield a lift-drag ratio equal to that of the biplane with all edge angles 7° when $C_{D,f}$ equals 0.00024. At an M_0 of 3.0, the biplanes with values of θ_L of 10° and 13° will equal the lift-drag ratio of the symmetrical biplane when $C_{D,f}$ is 0.00018 and 0.00041, respectively. These low values of $C_{D,f}$ indicate that under actual test conditions the unsymmetrical configuration will probably attain a higher lift-drag ratio than the symmetrical configuration.

OTHER TYPES OF BIPLANE

The use of circular convex sections in place of the triangular-section airfoils greatly increased the drag for a given thickness ratio t/c. For an M_0 of 3.0, an α of 0°, and a t/c of 0.088, for example, the drag coefficient C_D with circular convex sections

was found to be 0.0443 as compared with 0.0048 for the triangular-section biplane of the same thickness ratio. A biconvex single airfoil of the same thickness ratio has a C_D of 0.0146. No further calculations for curved-section biplanes were undertaken.

Another method of obtaining a partial pressure cancellation consisted in replacing the lower airfoil with a small shock-reflecting surface. (See fig. 12.) For this arrangement, C_L and C_D were estimated by means of graphical integration for an M_0 of 2.0, an α of 3°, and edge angles θ of 7°. As expected, the results are dependent on the ratio of the chord of the shock-reflecting surface to the chord of the airfoil L/c. The values obtained are:

L/c	C_D	C_L/C_D
0.25	0.031	4.67
.15	.029	5.58
.10	.028	5.69
.05	.027	5.58

Comparison with figure 8 shows that C_L/C_D does not approach the value obtainable with a diamond-profile airfoil. The drag coefficient, moreover, is about twice as great as for two symmetrical airfoils. For these reasons and because of its structural disadvantages, this scheme is probably of no practical interest. (For the airfoil of fig. 12 without the shock-reflecting surface, C_D is 0.028 and C_L/C_D is 5.20.)

CONCLUSIONS

From calculations of the aerodynamic coefficients of biplanes in a frictionless supersonic air stream, the following conclusions may be drawn:

1. For any given lift coefficient, a triangular-section biplane has lower drag than a diamond airfoil of the same thickness ratio.

2. When all edge angles are simultaneously varied, the lift-drag ratio increases as the angles are decreased.

3. With an upper airfoil of constant thickness, the maximum lift-drag ratio obtainable decreases as the thickness of the lower airfoil is increased. For low angles of attack, however, the lift-drag ratio of a biplane may be increased by making the lower airfoil thicker than the upper airfoil. If the lower-edge angles are too greatly increased, an optimum value is passed and the lift-drag ratio drops.

4. The lift-drag ratio of biplanes may be slightly improved by making the trailing-edge angles somewhat smaller than the leading-edge angles.

5. The variation of center of pressure with angle of attack is considerably greater for unsymmetrical than for symmetrical biplanes.

Inclusion of friction effects somewhat modifies the foregoing conclusions because the additional drag due to friction will be about twice as great for biplanes as for single airfoils. Calculations indicate that, as friction-drag coefficient increases, the thickness ratio of the lower airfoil of a biplane should be increased to maintain lift-drag ratios higher than those of symmetrical-diamond airfoils and that unsymmetrical biplanes will probably yield greater lift-drag ratios than symmetrical biplanes in frictional flows.

Certain practical disadvantages connected with biplanes should be considered in evaluating their practical usefulness. The spacing between the airfoils must be made variable if optimum performance is desired over a wide range of flight velocities. Over a certain limited range of flight Mach numbers, however, the biplane would maintain a higher lift-drag ratio than the diamond airfoil of the same thickness ratio. The greater loading of biplanes for a given lift can probably be dismissed as unimportant because it should be feasible to increase their strength by fastening the two airfoils together.

Flight Propulsion Research Laboratory,
    National Advisory Committee for Aeronautics,
        Cleveland, Ohio, December 10, 1946.

APPENDIX - DETERMINATION OF AERODYNAMIC

COEFFICIENTS OF SUPERSONIC BIPLANES

By use of the notation of figure 13, the pressure distributions over the biplane surfaces may be determined as follows: Upon entering field $(1, U)$ the air stream is turned through an angle $(\theta_{1,U} + \alpha)$ from the free-stream direction. The transition to field $(1, U)$ takes place through a compression shock. The angle $\varphi_{1,U}$ that this shock makes with the free-stream direction may be determined from oblique-shock relations. Similarly, upon entering field $(1, L)$ the flow is turned through an angle $(\theta_{1,L} - \alpha)$, also in a compressive sense, and the oblique shock makes an angle $\varphi_{1,L}$ with the free-stream direction. The resulting pressures in fields $(1, U)$ and $(1, L)$ may be obtained either from oblique-shock relations or, if $(\theta_{1,U} + \alpha)$ is fairly small, they may be closely approximated by the Prandtl-Meyer relations for flow around a corner. The Prandtl-Meyer relations are plotted in figure 4. Thus, for example, if M_0 is 2.0, $\theta_{1,U}$ is 7°, and α is 3°, $p_{1,U}/P$ is obtained by subtracting 10° from the turning angle Ψ corresponding to an M_0 of 2.0; that is, $\Psi_{1,U} = 26.3^O - 10^O = 16.3^O$; $p_{1,U}/P = 0.218$.

At the intersection of the two shocks from the leading edges, both shocks are deflected and the flow passes into a common field (U, L). The angle $\varphi_{2,U}$ that the shock makes with the flow direction in field $(1, U)$ is now determined from the known $M_{1,U}$ and the angle of deflection through the shock. The angle of deflection, in turn, is determined by the requirement of a common flow direction in field (U, L). This common direction can be attained only if the sum of the deflections through the two upper shocks equals the sum of the deflections through the two lower shocks. The deflection through the second upper shock is therefore $(\theta_{1,L} - \alpha)$ degrees and through the second lower shock is $(\theta_{1,U} + \alpha)$ degrees. The flow in field (U, L) has been turned $(\theta_{1,U} + \alpha + \theta_{1,L} - \alpha)$ degrees in a compressive sense and the conditions in field (U, L) can now be read from figure 4. Although the turning is compressive through both shocks, its direction is reversed and the actual flow direction in field (U, L) is $\lambda_{U,L} = (\theta_{1,U} + \alpha) - (\theta_{1,L} - \alpha) = (\theta_{1,U} - \theta_{1,L} + 2\alpha)$ degrees from the free-stream direction.

In passing into field $(2, U)$ the flow is expanded $(\theta_{2,U} - \alpha + \lambda_{U,L})$ degrees from its direction in field (U, L). The flow in field $(2, L)$ is expanded $(\theta_{2,L} + \alpha - \lambda_{U,L})$ degrees. The expansions take place through a wedge-shaped region with limits

determined by the values of β corresponding to the conditions before and after the expansion. The conditions are again obtainable from figure 4 because the turning angles are known.

The expansion waves are mutually deflected in the region of intersection. The angles that the bounding Mach lines beyond the interaction zone make with the flow direction are again determined by the conditions before and after the expansions. The angle of the line closing off field (2, U), for example, is $\left[\sin^{-1}(1/M_{2,U}) + (\theta_{2,U} - \alpha)\right]$. The angle of the line terminating the upper expansion region is determined by the number of degrees from field (2, U) that the flow is turned by the expansion wave. Each expansion wave is reflected from the surface and passes outside the airfoils. The four shocks emanating from the two trailing edges bring the entire flow pattern back to free-stream conditions at infinity. The angles of these shocks can be determined from this requirement (that is, free-stream conditions at infinity), but this determination is unnecessary to find the aerodynamic coefficients, for conditions beyond the trailing edges have no effect on the biplane.

In order to integrate the pressures over the airfoil surfaces, the continuous expansion waves are replaced with a succession of Mach waves, each of which turns the flow through a small angle $\Delta\theta$. Throughout this investigation the value $\Delta\theta$ was fixed at 1°. The problem of integration is obviously simple except over the portions of the inner rear surfaces that intercept the expansion waves from the opposite airfoil. This region may be treated analytically, by obtaining expressions giving the point at which each of the succession of Mach waves intersects the opposite surface. A summation process can then be made to determine the drag and lift forces contributed by these regions.

The relations between the angles of the Mach lines and their intercepts on the airfoil surfaces may be deduced from the sine law. The assumption is made that the bending of each Mach line through the interaction region takes place entirely at the point where it intersects the corresponding Mach line emanating from the opposite airfoil. The following expressions are obtained by using the notation of figure 14:

$$D_U = \frac{c_{1,U}}{\cos\theta_{1,U}} \frac{\sin(\varphi_{1,U} - \theta_{1,U} - \alpha)\sin(\varphi_{2,U} - \theta_{1,U} - \alpha)}{\sin(\varphi_{1,U} + \varphi_{2,U} - \theta_{1,U} - \alpha)} \qquad (1)$$

$$D_L = \frac{c_{1,L}}{\cos\theta_{1,L}} \frac{\sin(\varphi_{1,L} - \theta_{1,L} + \alpha)\sin(\varphi_{2,L} - \theta_{1,L} + \alpha)}{\sin(\varphi_{1,L} + \varphi_{2,L} - \theta_{1,L} + \alpha)} \qquad (2)$$

$$F_L = \frac{D_U + D_L}{1 + \dfrac{\tan \beta_{1,U}}{\tan \beta_{1,L}}} \tag{3}$$

$$F_U = F_L \frac{\tan \beta_{1,U}}{\tan \beta_{1,L}} \tag{4}$$

$$L_U = F_U \frac{\sin(\beta_{1,U} + \beta_{2,U})}{\sin \beta_{1,U} \sin(\beta_{2,U} - \theta_{2,U} + \alpha)} \tag{5}$$

$$L_L = F_L \frac{\sin(\beta_{1,L} + \beta_{2,L})}{\sin \beta_{1,L} \sin(\beta_{2,L} - \theta_{2,L} - \alpha)} \tag{6}$$

where

D   distance from shock intersection to inner turning corner

F   distance from intersection of expansion waves to inner turning corner

L   distance from inner turning corner to intersection of expansion wave with biplane surface

In each case β is the angle that the Mach lines make with the free-stream direction; that is, it is the Mach angle plus the angle which the local flow makes with the free-stream direction. Because the flow direction changes 1° through each Mach line, the expansion process must be followed quite carefully to determine the correct values of β to use in equations (3) to (6). When more Mach lines emanate from one of the airfoils, supplementary Mach lines may be assumed to emanate from the opposite airfoil in order that the bending points of the excess lines may be determined from equations (3) to (6).

When the intercepts of the Mach lines on the airfoil surfaces are known, the aerodynamic coefficients per unit span are obtained by a summation of pressures over the surfaces.

The course of the expansion may be clarified by studying the example of figure 2. Here the values of Ψ to be used in figure 4 and the direction of the flow λ are indicated in each region. The conditions $M_0 = 2.0$, $\theta_{1,U} = \theta_{2,U} = 7^\circ$, $\theta_{1,L} = \theta_{2,L} = 10^\circ$, and $\alpha = 3^\circ$ were assumed for this sketch.

The analytical method just described is useful only when the
shocks from the leading edges intersect the opposite airfoil at the
inner turning corner. If the coefficients for other cases are
desired, a graphical integration must be made or some other analytical
expressions derived. Graphical integration was used in the present
investigation to determine the effect of varying the Mach number while
a fixed biplane spacing was maintained and to determine the coeffi-
cients for the convex-section biplane and for the single airfoil with
shock-reflecting surface.

REFERENCES

1. Busemann, A.: Aerodynamischer Auftreib bei Überschallgeschwin-
   digkeit. Luftfahrtforschung, Bd. 12, Nr. 6, Oct. 3, 1935,
   pp. 210-220.

2. Walchner, O.: Zur Frage der Widerstandsverringerung von Tragflügeln
   bei Überschallgeschwindigkeit durch Doppeldeckeranordnung.
   Luftfahrtforschung, Bd. 14, Nr. 2, Feb. 20, 1937, pp. 55-62.

3. Ferri, A.: Experiments at Supersonic Speed on a Biplane of the
   Busemann Type. British R.T.P. Trans. No. 1407, Ministry Aircraft
   Prod. (From Atti di Guidonia, No. 37-38, Oct. 11, 1940,
   pp. 517-557.)

4. Taylor, G. I., and Maccoll, J. W.: The Two-Dimensional Flow Around
   a Corner; Two-Dimensional Flow Past a Curved Surface. Vol. III
   of Aerodynamic Theory, div. H, ch. IV, sec. 5-6, W. F. Durand,
   ed., Julius Springer (Berlin), 1935, pp. 243-249.

5. Lighthill, M. J.: A Note on Supersonic Biplanes. R. & M. No. 2002,
   British A.R.C., 1944.
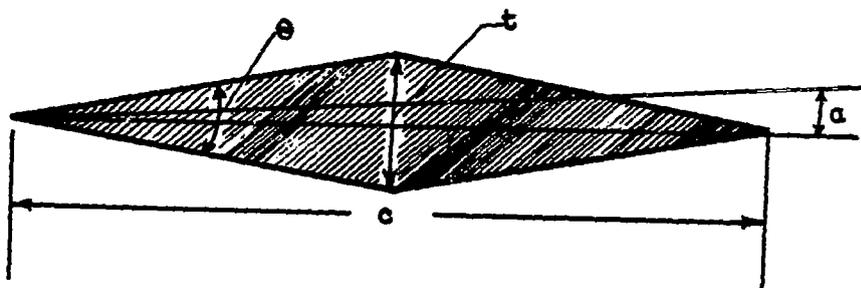
(a) Airfoil with diamond section.

Inner turning corners
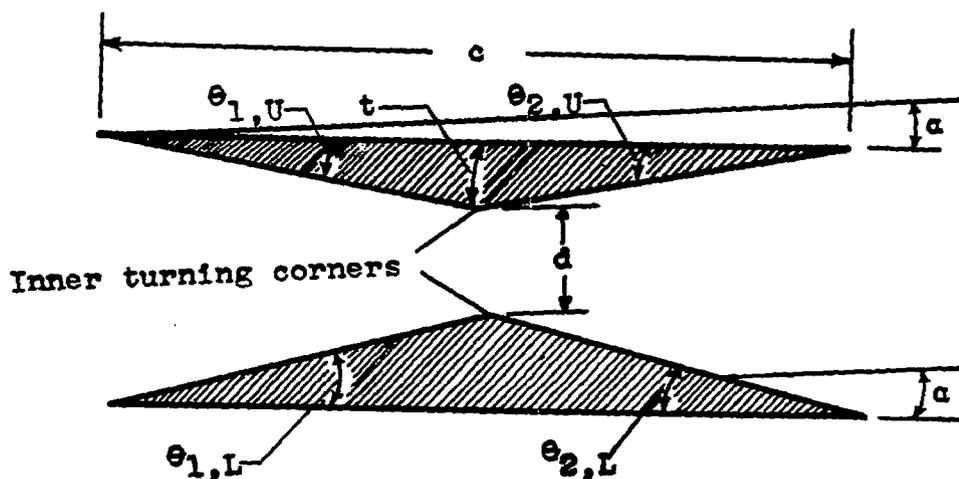
(b) Biplane with triangular sections.

Figure 1.— Geometry of diamond airfoil and triangular biplane.

Definitions of symbols:

θ edge angle
with subscripts:
   U   upper
   L   lower
   1   leading edge
   2   trailing edge
  α angle of attack

t maximum thickness (of thinner airfoil for biplane)
c chord of airfoil
d shortest distance between airfoils in biplane
t/c thickness ratio
d/c biplane spacing

Fig. 2
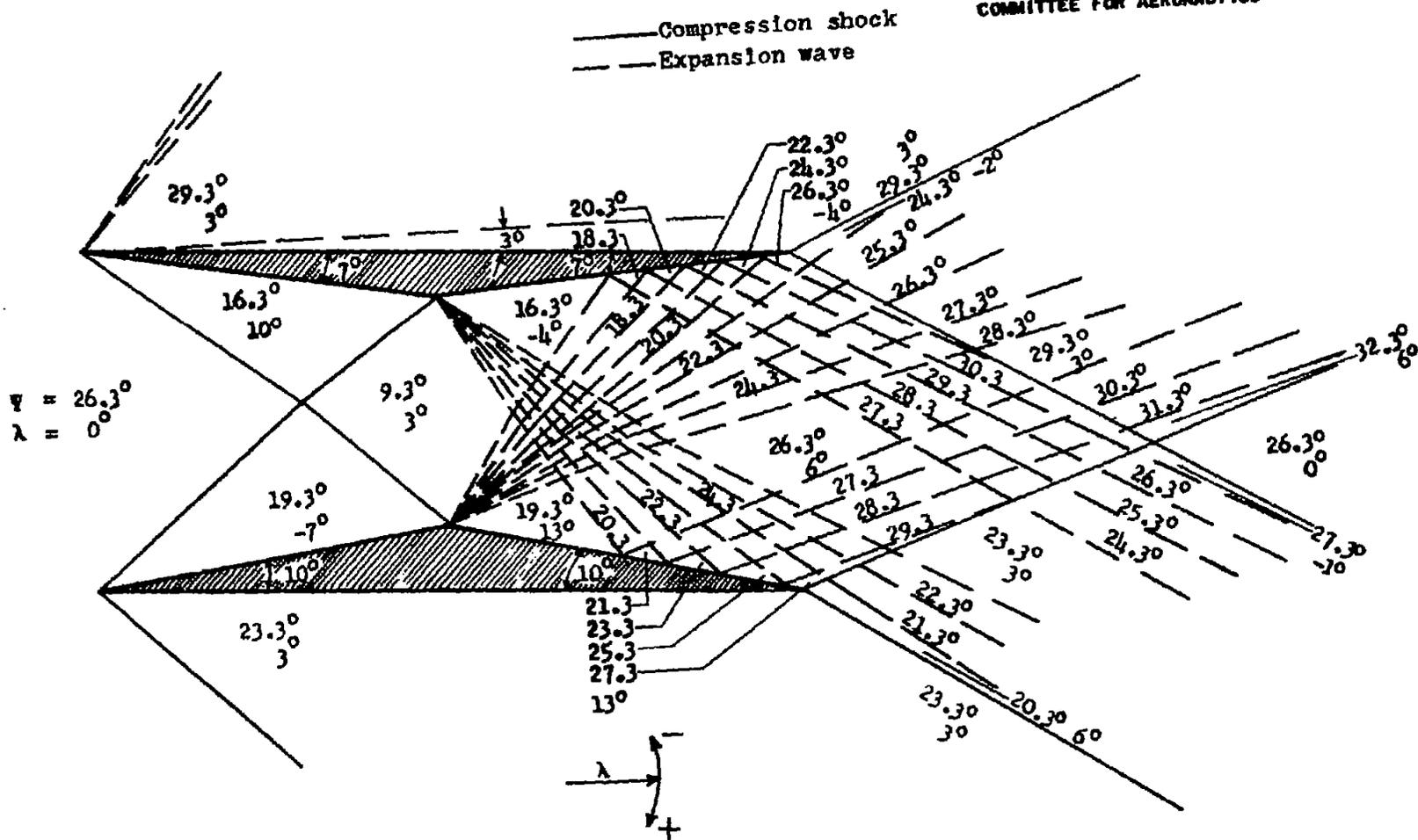
Figure 2.— Example of flow through triangular-section biplanes. Free-stream Mach number, M_0, 2.0. Ψ, angle through which flow is turned (Prandtl-Meyer theory); λ, angle between local flow direction and free-stream flow direction.

7.69
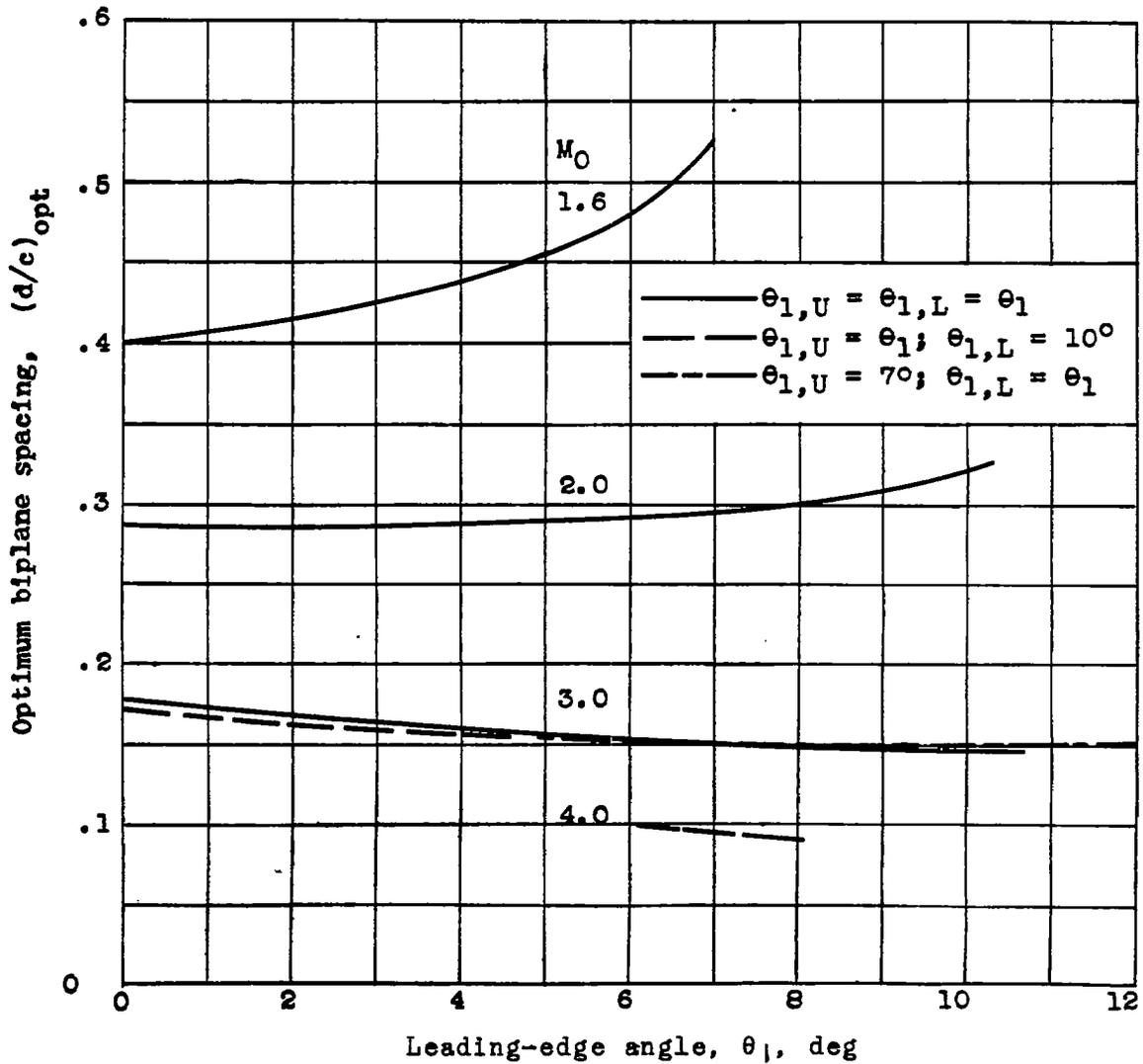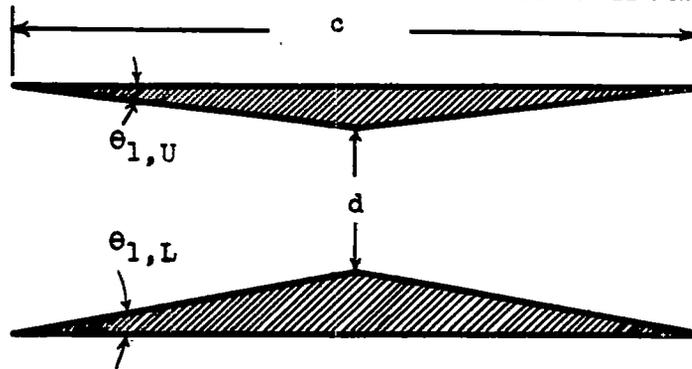
Figure 3. — Variation of optimum biplane spacing with leading-edge angles for several Mach numbers.

Fig. 4

NATIONAL ADVISORY
COMMITTEE FOR AERONAUTICS

$$\gamma = \frac{1}{k} \tan^{-1}(k\sqrt{M^2-1}) + \sin^{-1}\frac{1}{M} - 90^\circ$$

$$= \frac{1}{k} \tan^{-1}(k \cot \beta) + \beta - 90^\circ$$

$$\frac{p}{P} = \left[(1-k^2)\cos^2 k(\gamma - \beta + 90)\right]^{\frac{\gamma}{\gamma-1}}$$

$$k = \left(\frac{\gamma-1}{\gamma+1}\right)^{\frac{1}{2}}$$

$$\gamma = 1.40$$

β

p/P

M

Mach angle, β, deg

Pressure ratio, p/P

Mach number, M
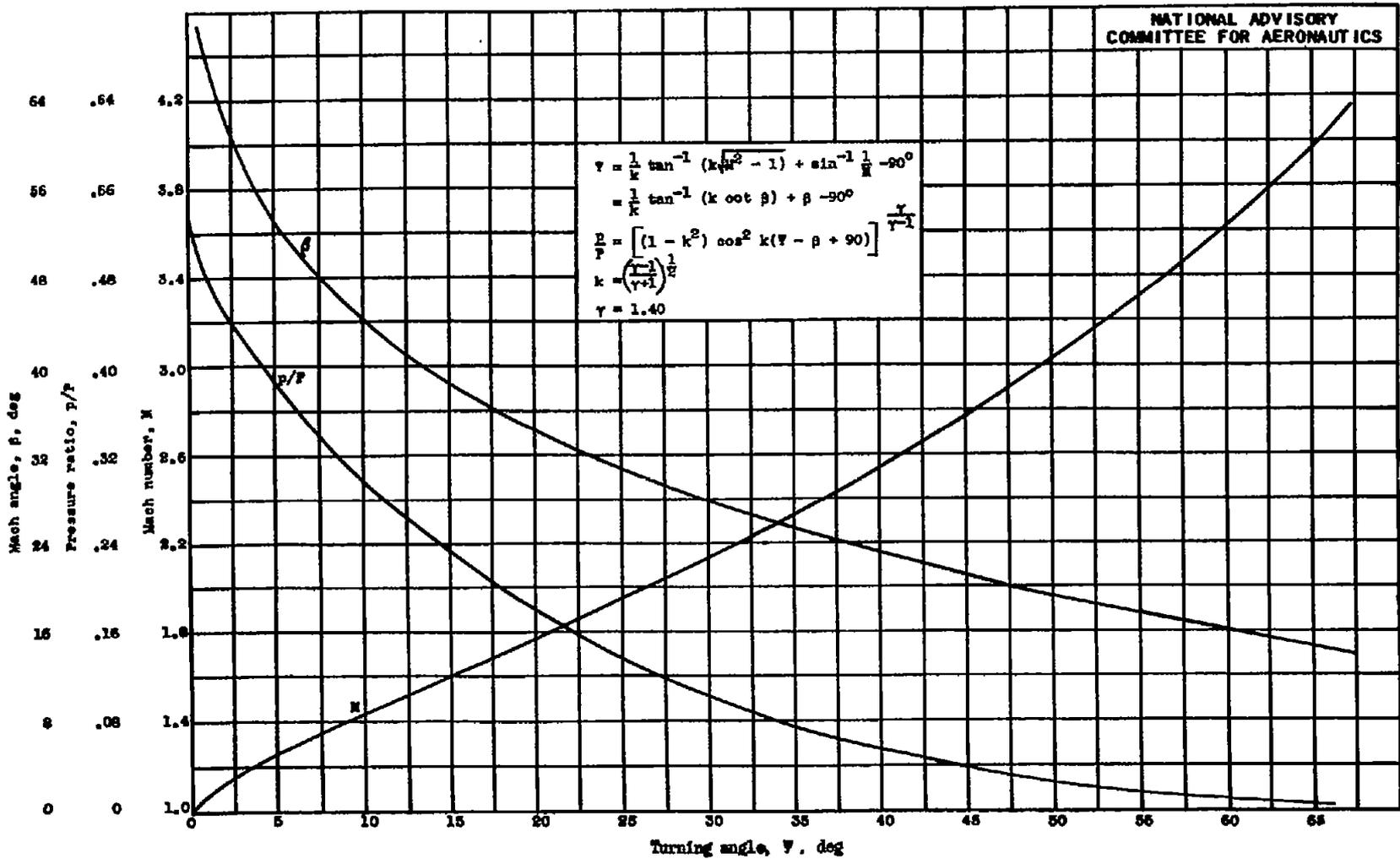
Turning angle, γ, deg

Figure 4.- Prandtl-Meyer relations for supersonic flow around corners. Mach number, Mach angle, and ratio of static to total pressure as functions of turning angle.
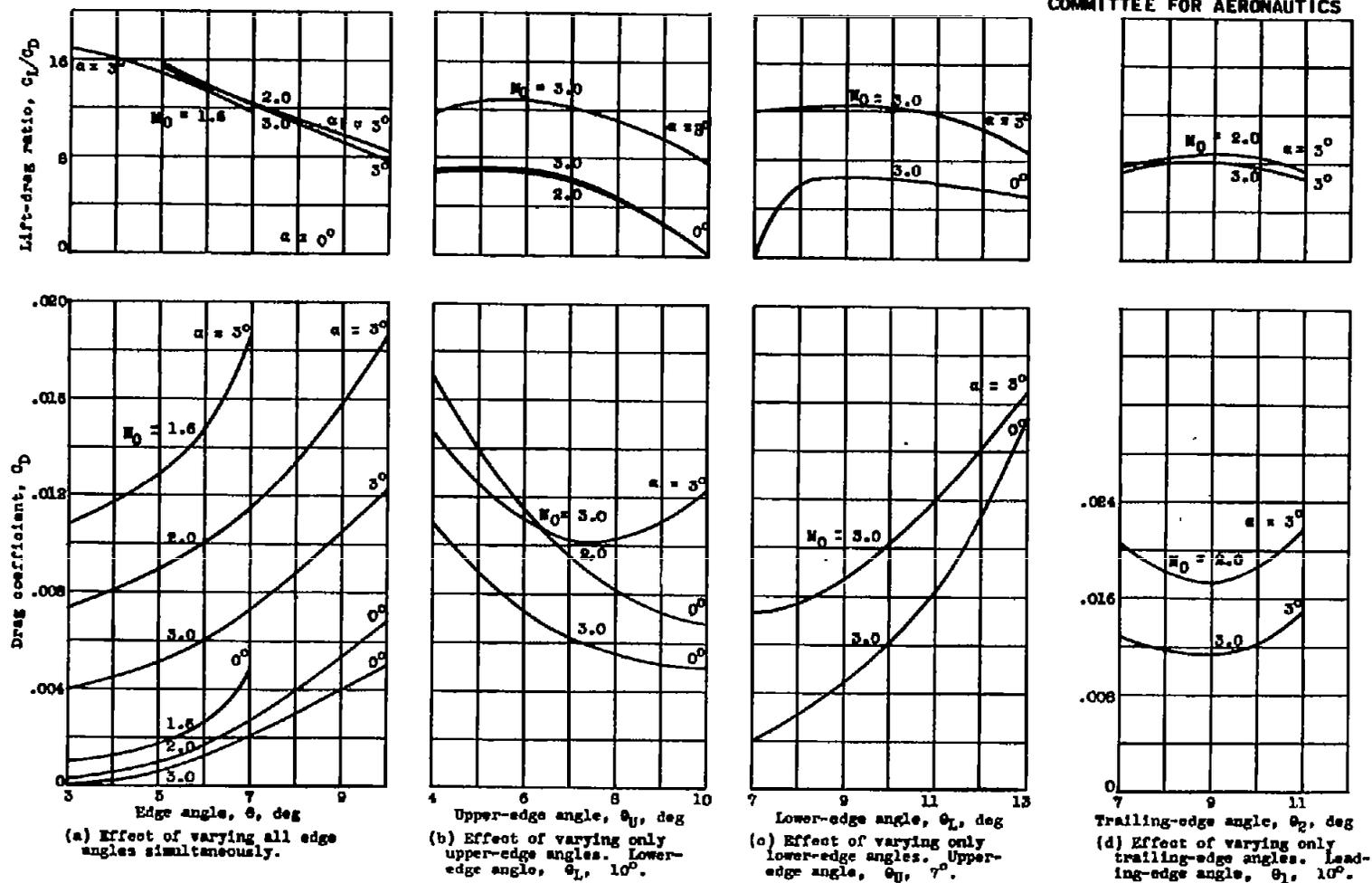
Figure 5.- Effect of varying edge angles on drag coefficient and lift-drag ratio of triangular-section biplanes.

Fig. 5

Fig. 6
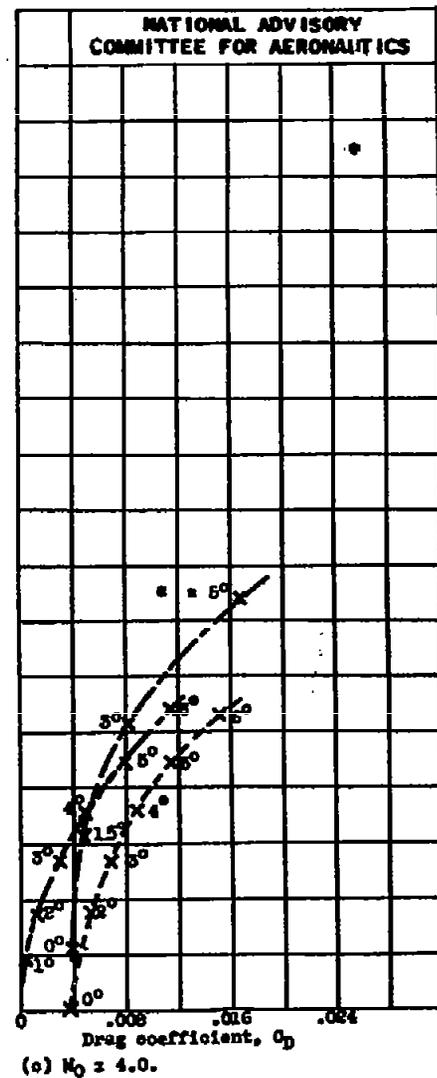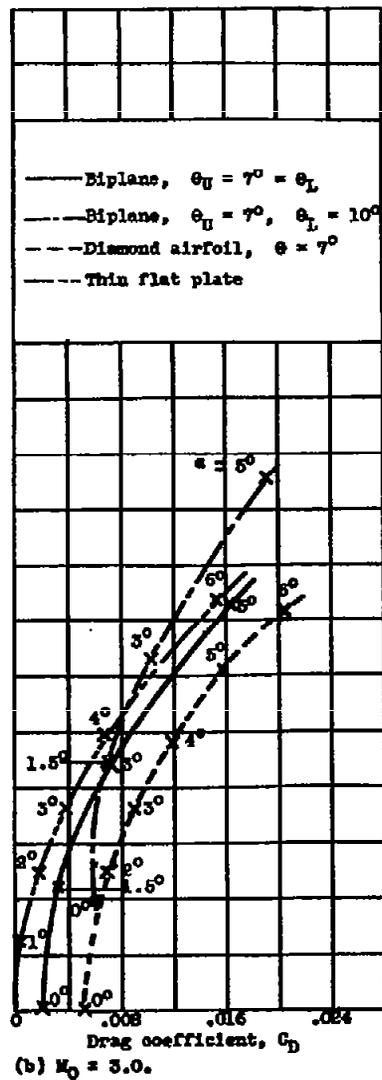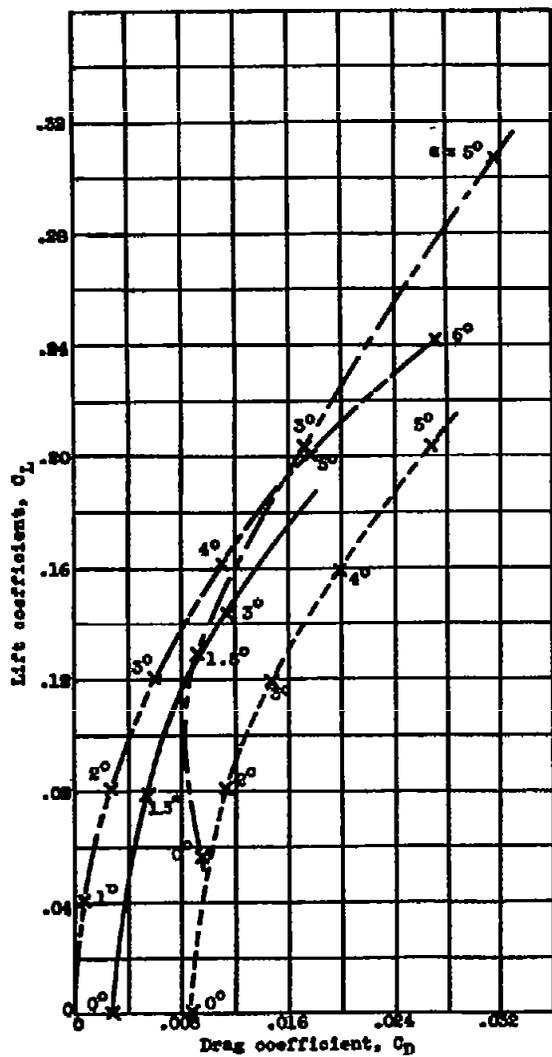
Figure 6.– Comparison of polar diagrams for a symmetrical and an unsymmetrical biplane, a symmetrical-diamond airfoil, and a thin flat plate at three Mach numbers.
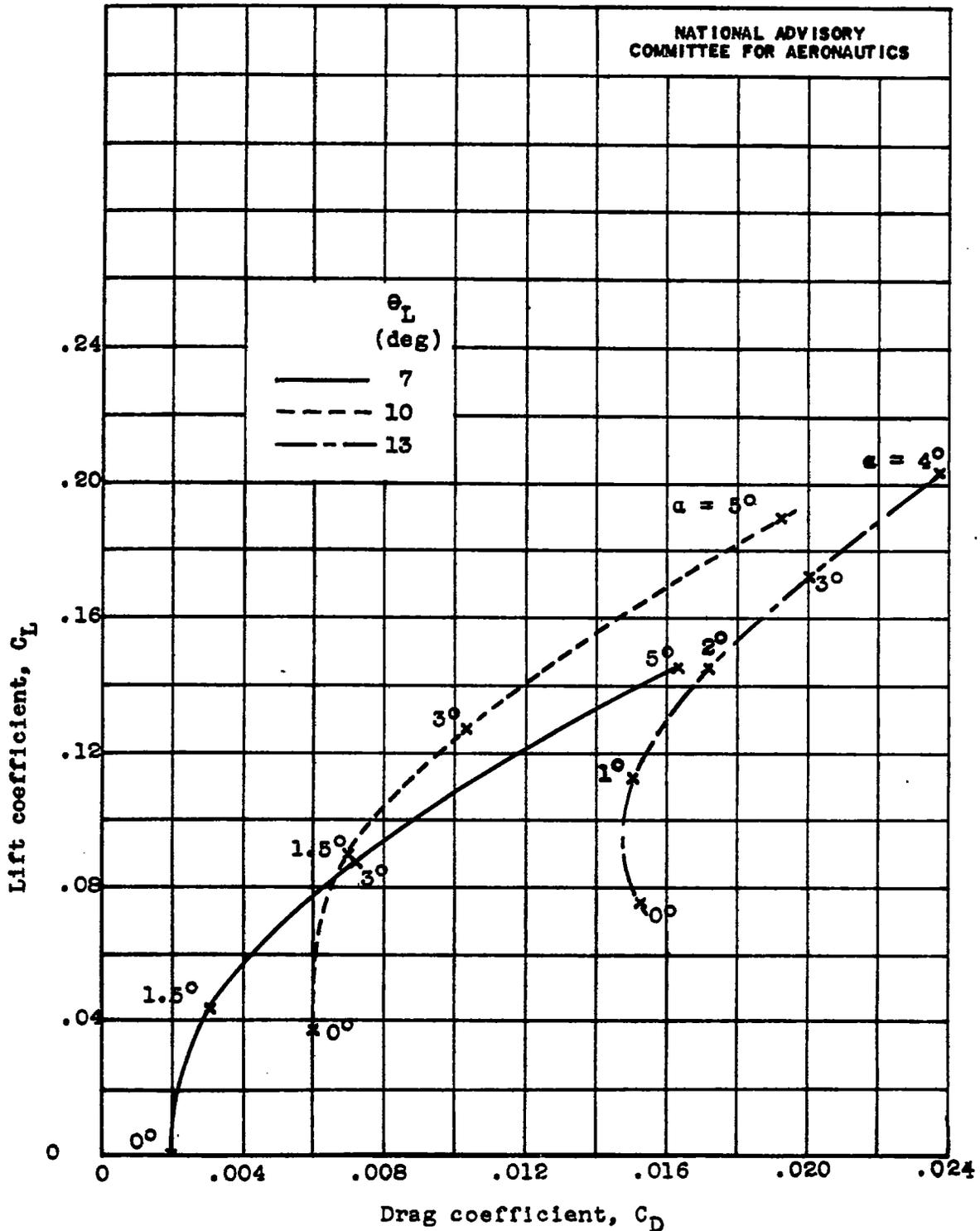
Figure 7.- Effect of increasing the lower-edge angles on polar diagram of triangular-section biplanes. Free-stream Mach number M_0, 3.0; upper-edge angle θ_U, 7°.

Fig. 8   NACA TN No. 1316
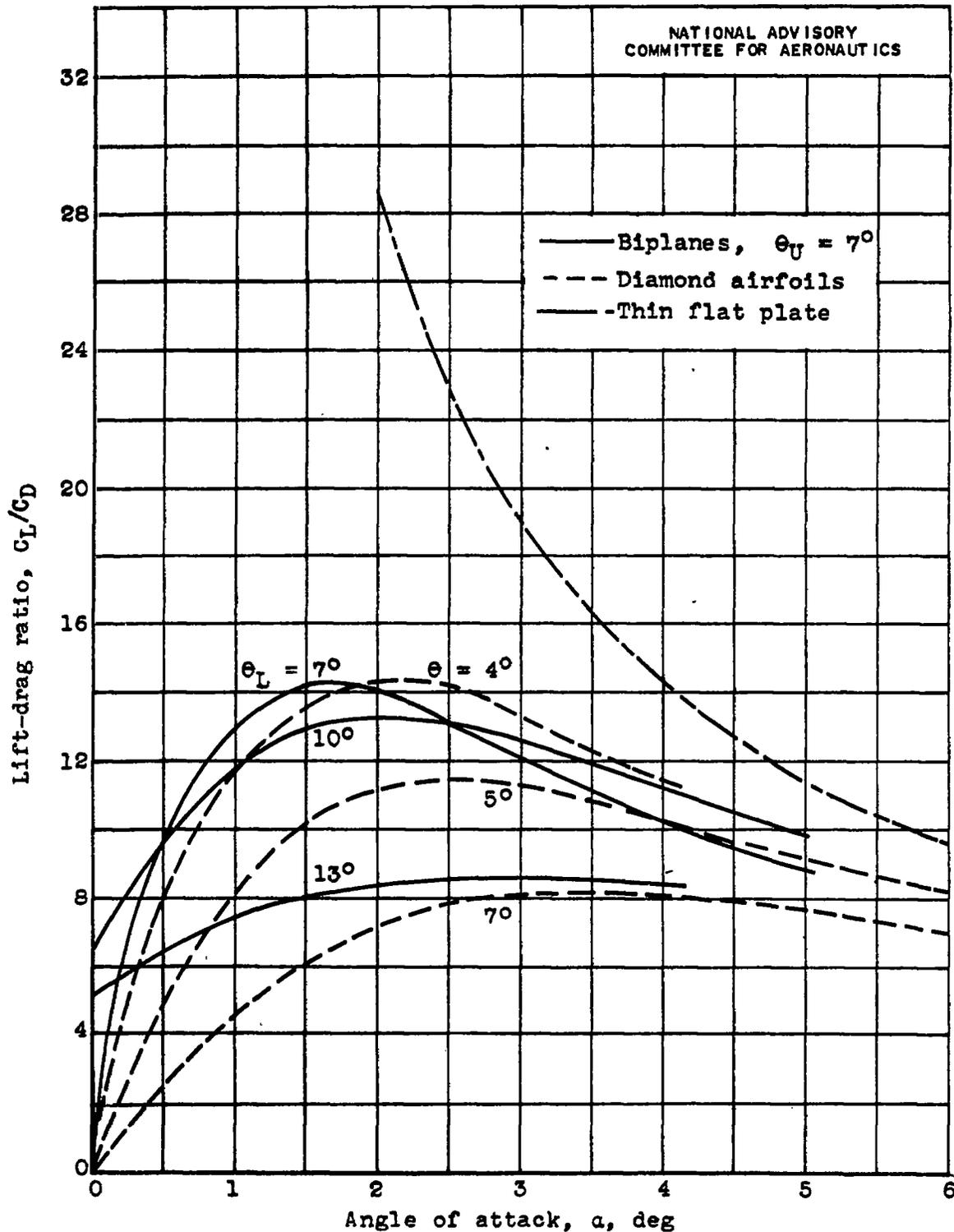
Figure 8.— Effect of edge angles on lift-drag ratio of
biplanes, diamond airfoils, and a thin flat plate. (For
definition of edge angles, see fig. 1.) Free-stream
Mach number M_0, 3.0.
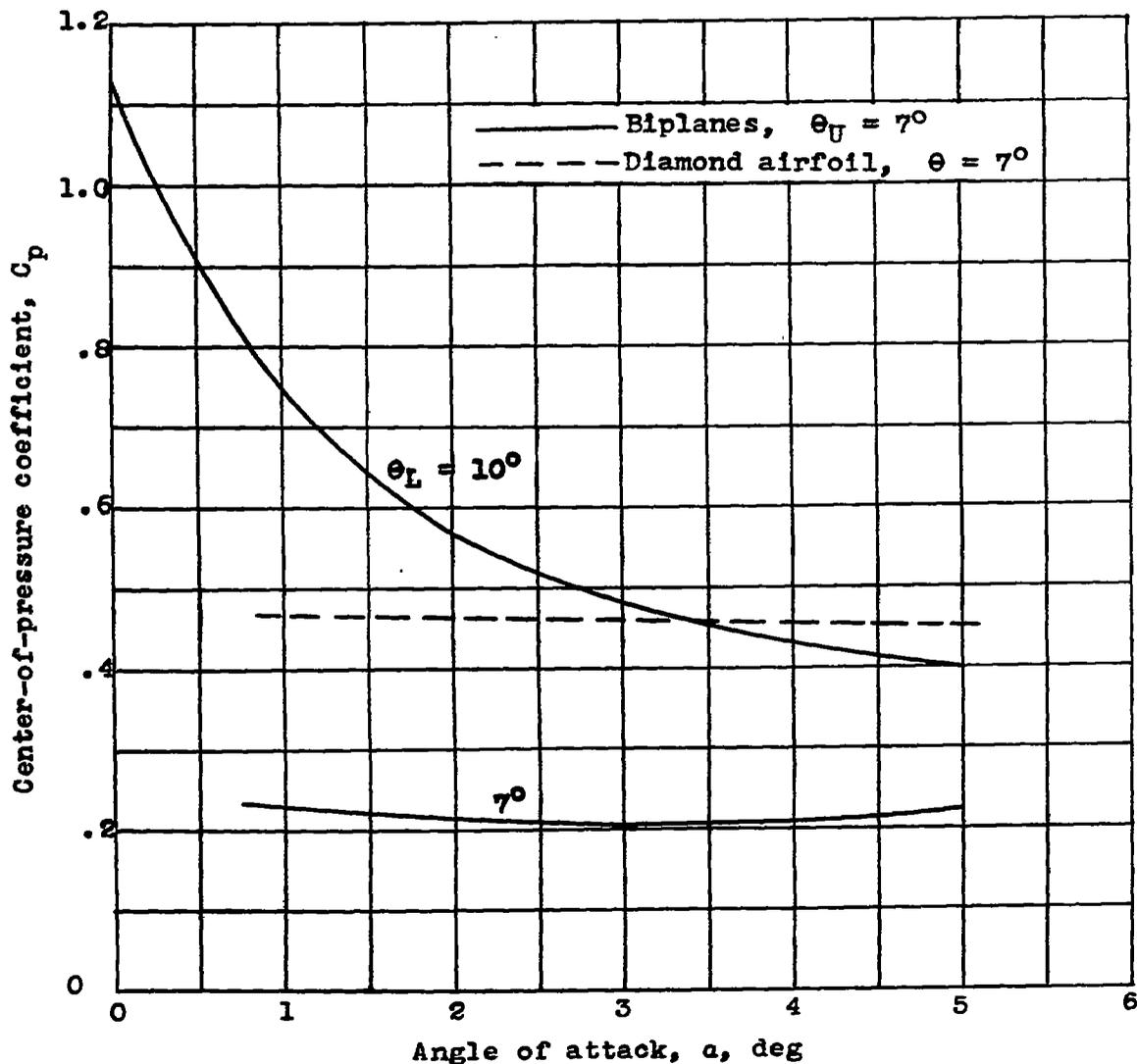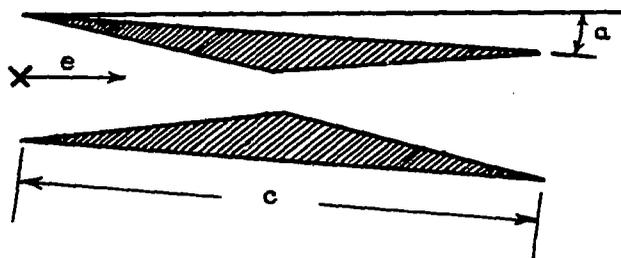
Figure 9.— Effect of angle of attack on center of pressure of
   two biplanes and a diamond airfoil.   (C_p = e/c.) Free-
   stream Mach number M_0, 3.0.

Fig. 10   NACA TN No. 1316
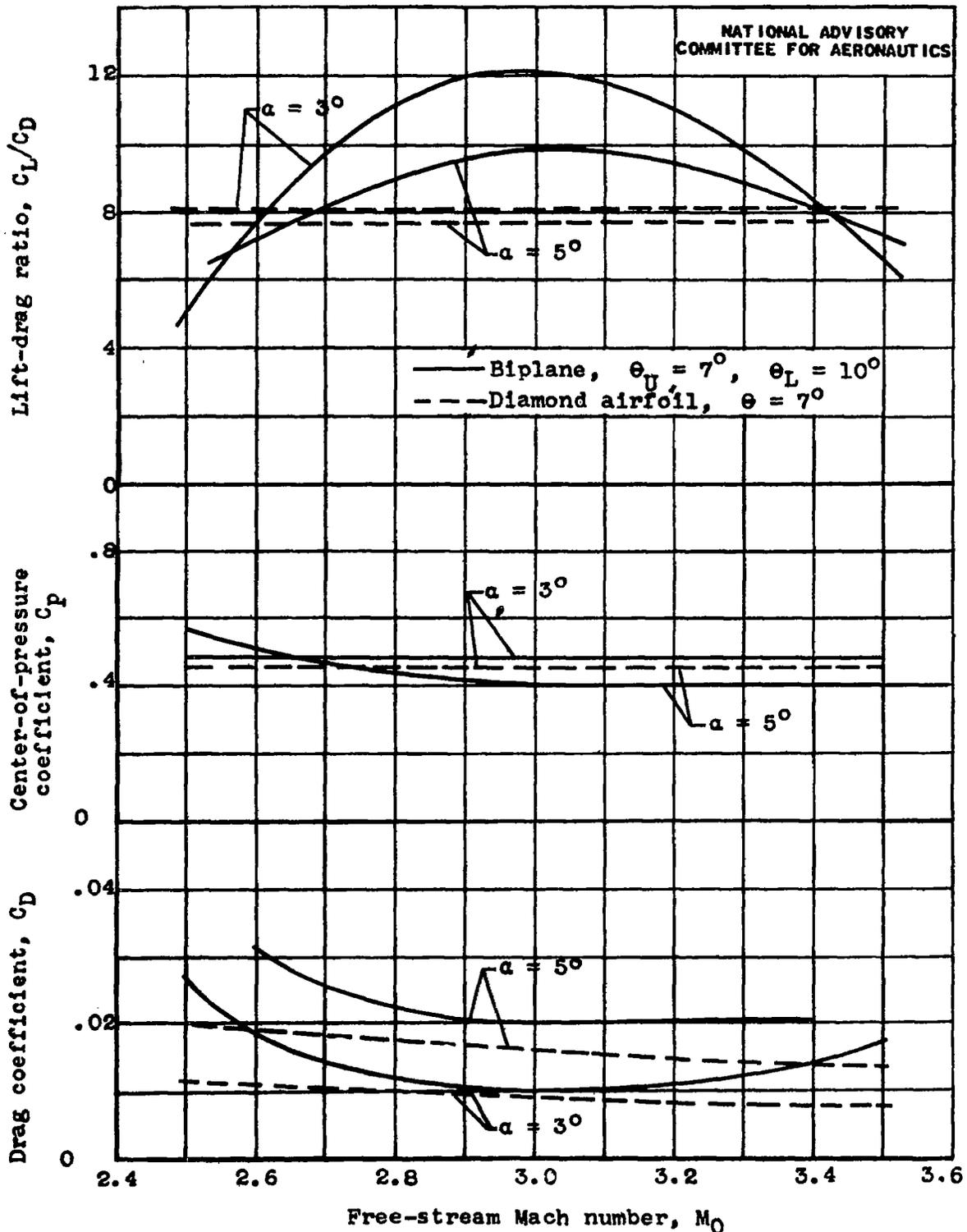
Figure 10.- Variation of drag coefficient, center of pressure, and lift-drag ratio with Mach number for biplane with optimum spacing for free-stream Mach number M_0 of 3.0. (d/c = 0.15.)
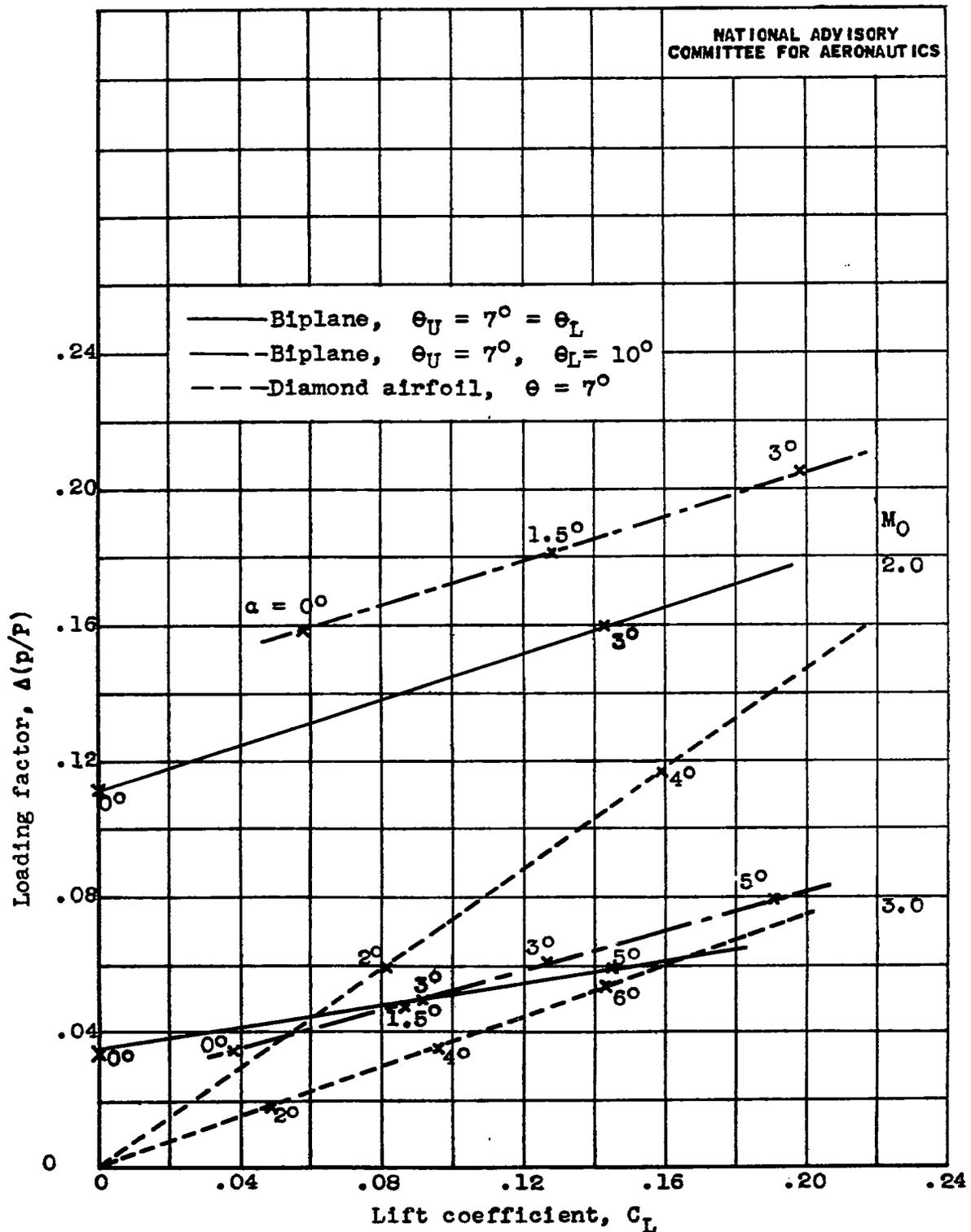
Figure 11.— Relation between lift coefficient and loading
factor for upper airfoils of two biplanes and for a diamond
airfoil at free-stream Mach numbers M_O of 2.0 and 3.0.
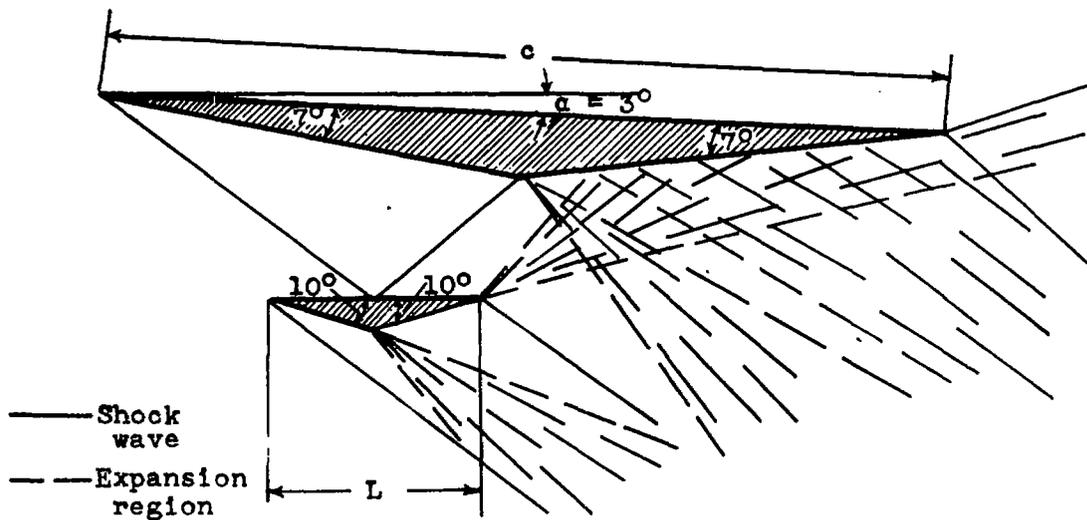
Figure 12.- Sketch of single triangular airfoil with shock-reflection surface. Free-stream Mach number M_0, 2.0.
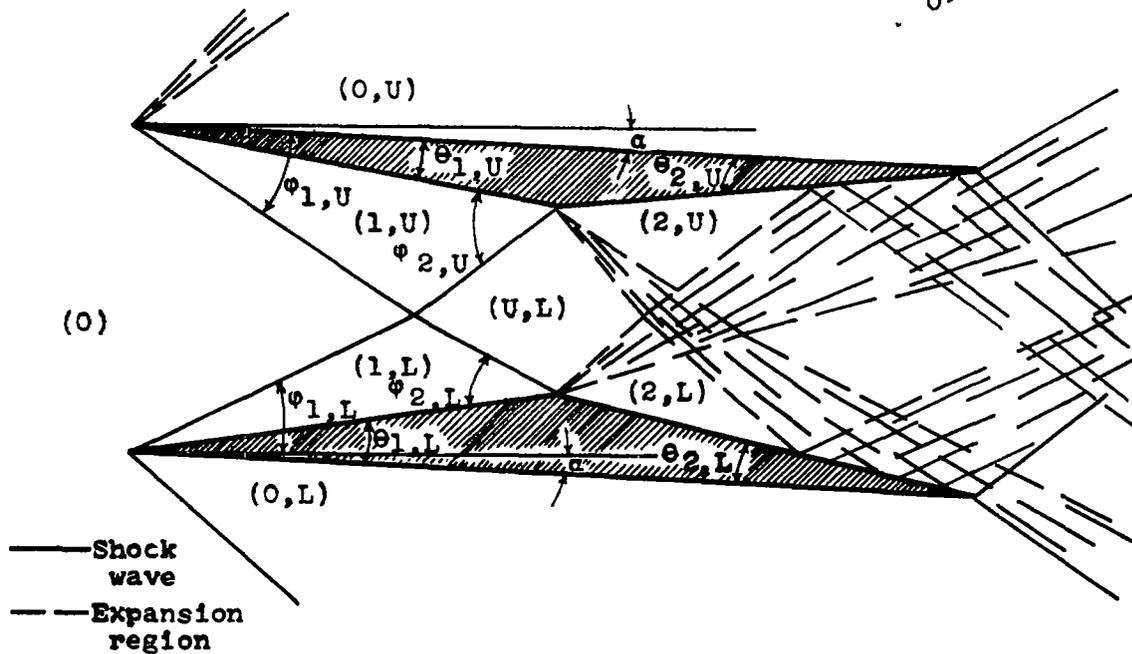
Figure 13.- Notation for analysis of flow through biplanes.
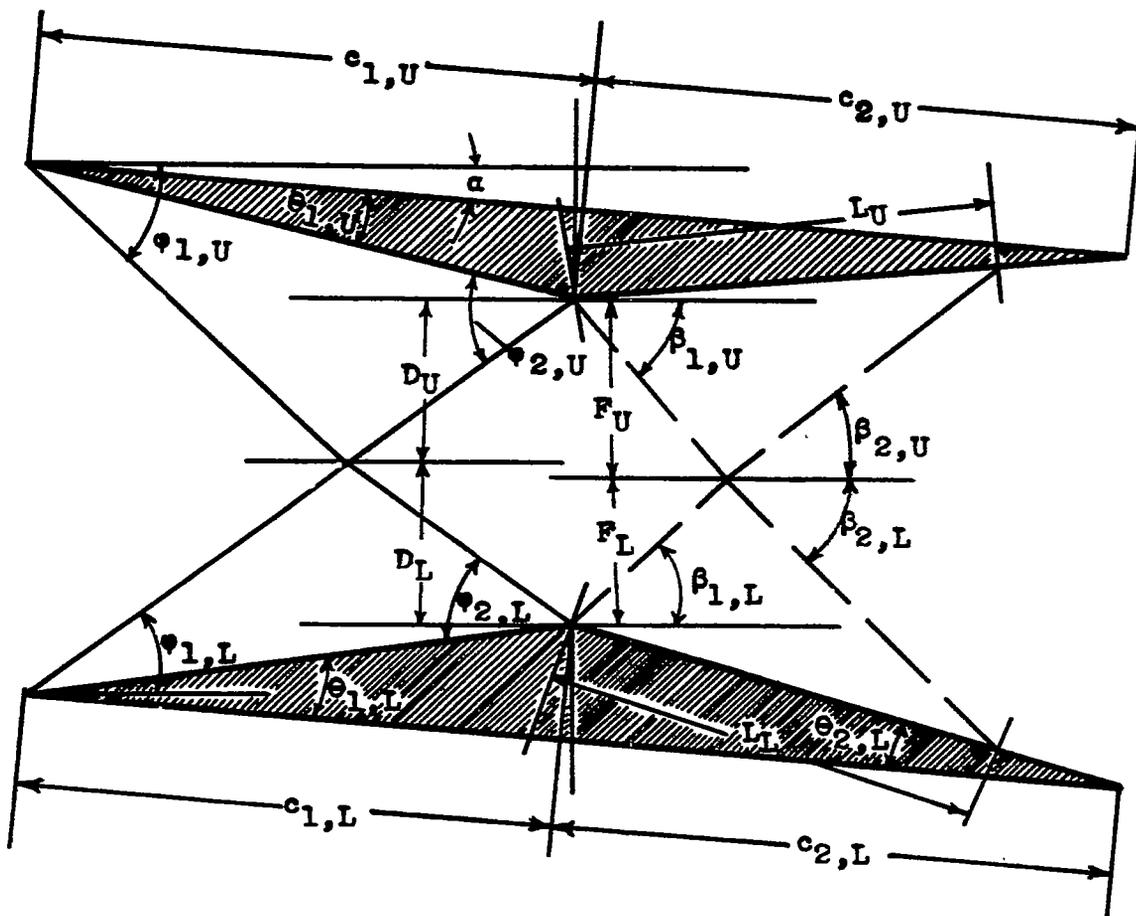
Figure 14.— Notation used for analytical integration process.